

Conformational studies and solution structure of laulimalide and simplified analogues using NMR spectroscopy and molecular modelling

Ian Paterson,* Dirk Menche, Robert Britton, Anders E. Håkansson and
María Á. Silva-Martínez

University Chemical Laboratory, Lensfield Road, Cambridge CB2 1EW, UK

Received 16 February 2005; accepted 22 March 2005

Available online 8 April 2005

Abstract—The solution structures of the potent microtubule-stabilizing anti-cancer agent laulimalide and simplified analogues were determined by a combination of high field ^1H NMR spectroscopic studies (*J*-based configuration analysis and NOESY) and constrained molecular dynamics simulations and discussed in relation to their antiproliferative activity.

© 2005 Elsevier Ltd. All rights reserved.

The marine macrolide laulimalide (**1**, Fig. 1)¹ represents an attractive lead compound for development as a new structural class of cancer chemotherapeutic agent. Lau-
limalide stabilizes microtubules in a similar manner to

Taxol® (paclitaxel) and inhibits the proliferation of a range of human carcinoma cell lines, including multi-drug and paclitaxel resistant cells, at low nanomolar concentrations.^{2,3} Moreover, it appears to have a different (and as yet undefined)⁴ binding site on tubulin^{5,6} and is much less susceptible to P-glycoprotein-mediated multidrug resistance.^{3a} This promising biological profile, together with its low natural abundance from its sponge sources, has triggered extensive synthetic efforts, culminating in a number of total syntheses of laulimalide.^{2,7,8} Despite these contributions, there is still a supply problem, which renders the development of structurally simplified and, as such, more readily accessible analogues an important goal. For the rational design of such analogues, an understanding of the detailed 3D structure and conformational behaviour of laulimalide should be highly informative.

While other microtubule-stabilizing agents have been extensively studied by analogue preparation and solution conformational analysis,⁹ no such detailed studies have been described for laulimalide and only a limited range of derivatives have been reported to date.⁸ So far, only the solid state structure (X-ray crystal structure of laulimalide itself) provides substantive information on the preferred conformation.^{1c} Herein, we report the elucidation of the solution structure of laulimalide (**1**), together with selected simplified analogues **2a–d** featuring a modified macrocyclic core at C11 and having a

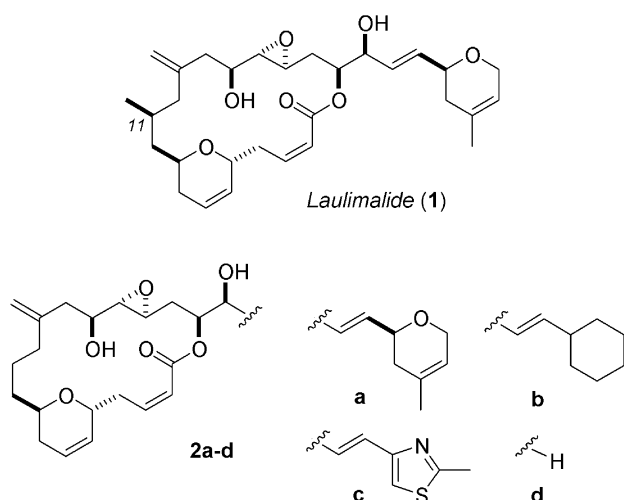


Figure 1. Lauimalide (**1**) and its 11-desmethyl-analogues **2a–d**.

Keywords: Lauimalide; Solution structure; Conformational analysis; Analogues; Anti-cancer agent; Modelling.

* Corresponding author. Tel.: +44 1223 336407; fax: +44 1223 336362; e-mail: ip100@cam.ac.uk

truncated or replacement side chain at C20,^{8g} by ¹H NMR spectroscopy and molecular modelling.

The salient structural features of laulimalide include a 20-membered macrolide ring, two dihydropyran units, an epoxide, five double bonds and nine stereogenic centres. As a close mimic of biologically relevant systems, all spectral data for laulimalide were recorded in CD₃OD¹⁰ in a similar manner to our recent conformational studies on dictyostatin, a related microtubule-stabilizing marine macrolide.^{9c} Optimum ¹H NMR signal dispersion was realized at the highest available field strength (700 MHz), allowing the complete assignment of all resonances.¹¹ A combination of multiplet analysis,¹² homonuclear decoupling and TOCSY experiments at different mixing times (Fig. 2) was used for the extraction of all ³J_{H,H} coupling constants, while information on the spatial relationships between nonadjacent protons was deduced from NOESY experiments (0.5 s mixing time). Based on these data, laulimalide was divided into three subunits—a ‘northern’ (C13–C19, Fig. 2a) and ‘southern’ (C1–C12, Fig. 2b) region of the macrocycle, and the side chain (C19–C27, Fig. 2c).¹³

The northern (C13–C19) region (Fig. 2a) is characterized by a sequence of small/large coupling constants and distinctive NOESY data, indicating the relative rigidity within this subunit. In particular, small couplings observed for H-15 to H-16, H-17 to H-18a and H-18a to H-19 suggest *gauche* relationships between these protons. The large couplings for H-15 to H-14a and H-18b to both H-17 and H-19, in combination with a strong NOESY interaction between H-17 and H-19, led to the conformational assignment for the C15–C19 region as shown. Based on this analysis, the epoxide ring is expected to be on the outside of the macrocycle. The predominance of this conformer is further supported by a number of additional NOESY correlations (e.g., H-14b to H-15, H-16 to H-18b).

Conformational assignment of the southern region of laulimalide (Fig. 2b) was based on a combination of NOESY data (H-5 to H-3 and H-4b to H-6) and a large vicinal coupling between H-5 and H-4a. The *gauche* relationship between H-5 and H-4b (³J_{H,H} = 2.9 Hz) supports this assignment. A strong NOESY correlation from H-3 to H-5, together with a large dipolar coupling

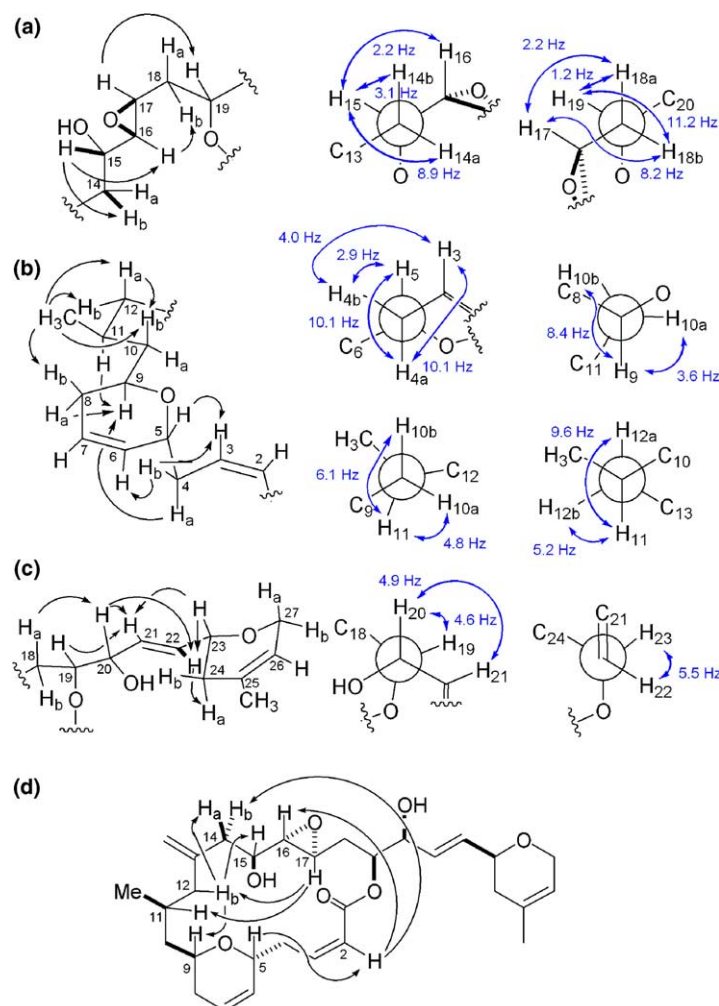


Figure 2. Laulimalide: selected NOESY correlations (single arrows) and ³J_{H,H} values (double arrows) within (a) the C14–C19 region; (b) the C2–C12 region and (c) the C18–C27 region; (d) transannular NOESY correlations.

of H-3 to H-4a, indicates that the *cis*-enoate protons are oriented on the same face as H-4b and H-5. A further NOESY correlation between H-4a and H-9 shows the spatial proximity of these protons. Although the coupling constants for the C9–C12 region reveal a continuation of small/large values for vicinal protons, the magnitude of these couplings indicates that the conformational bias for this region of the macrocycle is not as pronounced as that observed within the northern part. NOESY correlations between the CH₃ group at C11 and H-8b and H-11 and H-9, in combination with large couplings from H-10b to both H-9 and H-11, support a *gauche* relationship for C8 and C11 within this segment. The conformation depicted for the southern region in Figure 2b is further supported by both a large dipolar coupling from H-11 to H-10b and H-12a and a strong NOESY correlation between the latter protons.

Within the side chain (Fig. 2c), strong NOESY interactions between H-20 and H-18a and a small coupling to H-19 suggest a 1,3-diaxial relationship for H-20 and H-18 and a *gauche* relationship to H-19. The magnitude of the H-19 to H-20 scalar coupling suggests some flexibility within this region. Equally strong NOESY correlations were observed from both H-20 and H-23 to the two olefinic protons (H-21 and H-22), indicating (in combination with a H-22/H-24a/b NOESY correlation) that H-20 and H-23 reside on the same face above the plane of the olefin. The observed large coupling constants for H-20 to H-21 and H-22 to H-23 support this analysis.

For defining the relative orientation between the northern and southern subunits, a series of transannular NOESY interactions proved valuable (Fig. 2d). Of particular note, a correlation from H-2 to H-5, H-16 and H-14a, suggested these protons reside on the same upper face of the macrocyclic ring. Following this argument, protons H-9, H-11, H-12b, H-14a, H-15 and H-17 are expected to be located on the other (lower) side of the ring in the predominant conformation. No NOESY interaction between the side chain segment (C20–C28) and the macrocyclic core were observed.

On the basis of this spectroscopic analysis, files with constrained torsion angles and distances were generated in MacroModel 8.0¹⁴ and subjected to restrained Monte Carlo 10,000 step conformational searches (MM2 force field) with the generalized Born/surface area (GB/SA) water solvent model.¹⁵ These calculations revealed conformation **1-conf 1** (Fig. 3a and b) as the global minimum conformation in solution, within a series of discrete families of structurally closely related low energy conformations within 2 kcal mol^{−1}, as shown in the overlay in Figure 3c (**1-conf 1** in green, **1-conf 2** in red: +0.7 kcal mol^{−1}, **1-conf 3** in blue: +1.4 kcal mol^{−1}). This lowest energy conformation is closely related to the known solid state structure of laulimalide.^{1c,16} It adopts an open and flattened gross conformation (Fig. 3a and b). The side chain, the unsaturated C2/C3- and C21/C22-segments, as well as the epoxide moiety, are within the same plane, while the dihydropyran unit in the macrocycle is bent below. Notably, the relative proximity

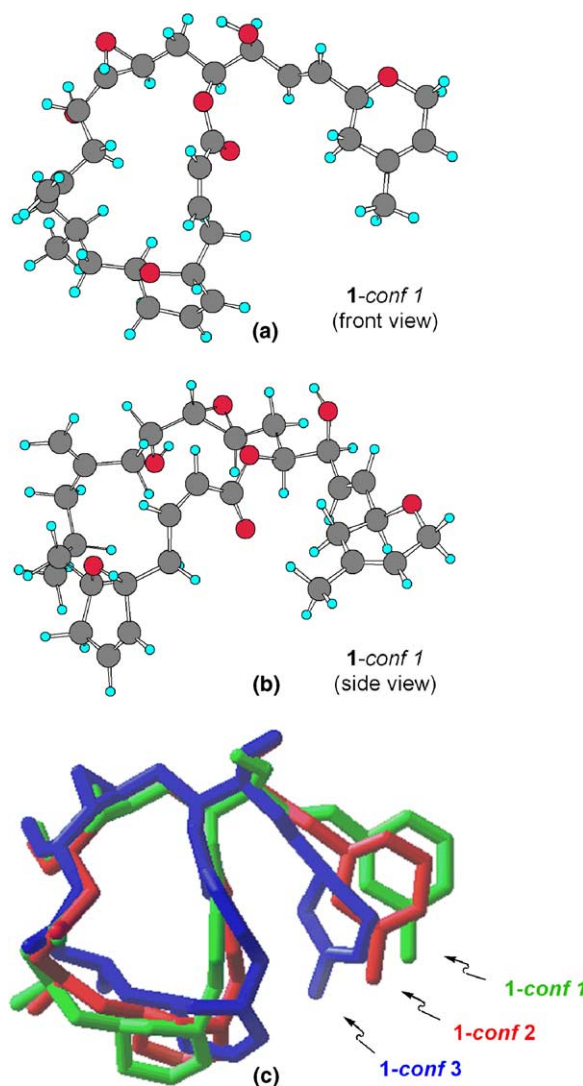


Figure 3. Global minimum conformation of laulimalide in solution as obtained from (a, b) constrained molecular dynamics simulation and (c) overlay of selected conformers within 2 kcal/mol of the global minimum.

and orientation of C17 and the C20–OH account for the well documented facile nucleophilic opening of the epoxide by the side chain hydroxyl group to produce isolaulimalide.^{1b,7c}

Comparing the low energy conformations (Fig. 3c) reveals the C14–C20 and the C1–C3 region to be relatively rigid. Interestingly, this segment has previously been suggested to be part of the pharmacophore region of laulimalide,^{8d} as any structural modifications within this region have led to a considerable loss of antimitotic potency.⁸ The C9–C12 subunit, as well as the side chain, in contrast, appears to be conformationally more flexible.

Based on a novel synthetic approach,^{8d,17} we have recently prepared the series of 11-desmethyl-laulimalide derivatives **2a–d**, as a first entry into structurally simplified analogues.^{8d,g} In particular, 11-desmethyl-laulimalide (**2a**) was shown to be similar in biological potency to laulimalide, while microtubule-stabilizing properties

Table 1. Selected $^3J_{\text{H,H}}$ coupling constants for laulimalide (**1**) and analogues **2a–d**

	1	2a	2b	2c	2d
H-3 to H-4a	10.1	10.4	10.4	10.4	10.3
H-3 to H-4b	4.0	3.4	3.5	3.5	3.3
H-4a to H-5	10.1	10.1	10.7	10.8	10.6
H-4b to H-5	2.9	3.1	3.0	2.1	2.6
H-9 to H-10a	3.6	2.7	3.1	2.5	2.9
H-9 to H-10b	8.4	8.6	8.3	8.2	8.6
H-10a to H-11a	4.8	5.4	5.5	4.9	6.2
H-10a to H-11b	n.a.	6.6	6.8	7.1	6.7
H-10b to H-11a	6.1	6.3	6.9	6.9	6.6
H-10b to H-11b	n.a.	6.7	6.4	7.2	6.6
H-11a to H-12a	9.6	8.9	8.5	9.2	~7
H-11a to H-12b	5.2	5.6	4.9	4.8	~7
H-11b to H-12a	n.a.	5.7	n.d.	n.d.	~7
H-11b to H-12b	n.a.	9.3	n.d.	n.d.	~7
H-14a to H-15	8.9	8.2	8.7	7.3	8.6
H-14b to H-15	3.1	3.2	3.9	3.7	3.9
H-15 to H-16	2.6	2.2	2.1	2.2	2.1
H-16 to H-17	2.5	2.2	2.2	2.2	2.2
H-17 to H-18a	2.2	3.6	3.9	3.1	4.6
H-17 to H-18b	8.2	7.9	7.3	7.9	7.5
H-18a to H-19	1.2	1.9	1.9	1.8	2.2
H-18b to H-19	11.2	11.3	11.4	11.3	11.0
H-19 to H-20	4.6	4.4	4.7	4.7	4.8

n.a.: not applicable.

n.d.: not determined due to signal overlap.

and antimitotic activity decreased markedly in the sequence **2a**, **2b**, **2d**, **2c**. In a similar analysis to that presented above (Fig. 2), all of these new analogues were extensively studied by high field ^1H NMR spectroscopy (700 MHz, CD_3OD),¹¹ revealing their close conformational resemblance to laulimalide. Selected coupling constants are depicted in Table 1, showing key data for the northern (rows 15–20, H-14a...H-20) and the southern regions (rows 1–14, H-3...H-12b) of the macrocycle, as well as for attachment of the side chain (row 21, H-19 to H-20).

The close similarity in magnitude of the coupling constants within the northern regions of all these compounds indicates this region to be conformationally rigid. Notably, the coupling constants observed for H-14 and H-15 (rows 15–17), which are closest to the methyl group deletion at C11, are practically identical. In addition, there was little effect of varying the side chain on the coupling constants observed within the C2–C5 (rows 1–4) and the C6–C10 (or southeastern) segments of the macrocycle. While the antimitotic potency of 11-desmethyl-laulimalide and the above observations suggest a similar solution conformation for these macrolides, a number of small deviations were observed. In particular, an increase in the magnitude of dipolar couplings between H-10a and H-11a and a decrease in the *antiperiplanar* couplings from H-11a to H-12a support a slight but noticeable loss in conformational bias. The favoured relative orientation of the side chain to the macrocyclic ring seems to be consistent for all the analogues **2a–d**, irrespective of their substituent, as indicated by the coupling constants H-19 to H-20, which is also supported by similar NOESY interactions to those discussed above for the parent compound **1**

(Fig. 2c). In the same way, a series of short and long range NOESY correlations support the strong conformational similarities within the macrocyclic core of laulimalide and its analogues.

In a similar way to that already described for laulimalide, molecular dynamics simulations were performed for analogues **2a–d** [Macromodel 8.0, 10,000 step Monte Carlo searches, MM2 force field, generalized Born/surface area (CB/SA) water solvent model] relying on previously generated input files with constrained torsion angles and distances as extracted from our spectral analyses. As expected from the closely related NMR data, very similar conformations were obtained. Figure 4a shows an overlay of the lowest energy conformation of 11-desmethyl-laulimalide, **2a-conf 1** in blue, with the higher energy conformation **2a-conf 2** in grey (+1.2 kcal mol^{−1}), which is closely related to the global minimum calculated for laulimalide, **1-conf 1** in green. Noticeable differences appear in the C10–C12 and the C2–C3 regions. As shown in Figure 4b for the overlay of the global minima of **2a** and its side chain analogues **2b–d**, substitution or truncation of the side chain has little influence on the preferred macrocyclic conformation.

In summary, based on extensive ^1H NMR spectroscopic studies and constrained molecular dynamics simulations, we have elucidated the dominant solution structures of laulimalide and a series of analogues, with both a simplified macrocycle (deletion of the 11-methyl group) and side chain (truncation or substitution). In solution, these macrolides adopt an open conformation similar to the solid state structure of laulimalide and are characterized by having a rigid C14–C19 segment and flexibility within both the C10–C12 region and the side

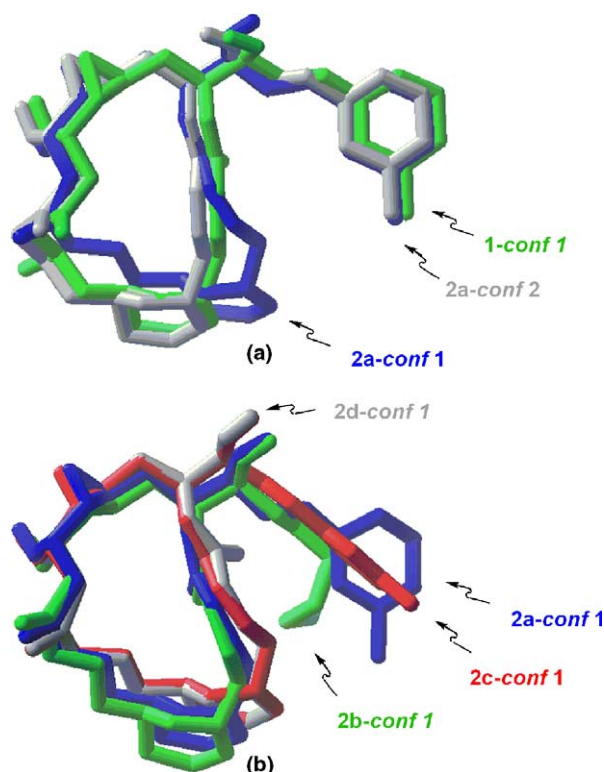


Figure 4. Solution conformation of 11-desmethyl-laulimalide (**2a**) in comparison to laulimalide (a) and to its side chain analogues **2b–d** (b).

chain. Deletion of the 11-methyl group, as in **2a**, only has a minor influence on the 3D structure, which is in agreement with the available biological data. Likewise, substitution or truncation of the side chain does not change the macrocyclic conformation but does significantly reduce the antimitotic potency,^{8g} indicating that this is an essential part of the pharmacophore region. Altogether, these results suggest that it is indeed possible to simplify the structure of laulimalide while retaining the overall shape and biological activity. A more challenging goal remains to retain potency and enhance chemical stability by designed modifications that constrain the more conformationally flexible areas within the laulimalide structure.¹⁸

Acknowledgements

We thank the European Commission (IHP Networks HPRN-CT-2000-18 and HPRN-CT-2000-00014; fellowship for D.M.), the EPSRC (GR/N08520), the NSERC-Canada (fellowship for R.B.) and Merck for financial support, and Dr. Jonathan Goodman (Cambridge) for assistance with the modelling studies.

Supplementary data

Supplementary data associated with this article can be found in the online version, at [doi:10.1016/j.tetlet.2005.03.149](https://doi.org/10.1016/j.tetlet.2005.03.149).

References and notes

- (a) Quinoa, E.; Kakou, Y.; Crews, P. *J. Org. Chem.* **1988**, *53*, 3642; (b) Corley, D. G.; Herb, R.; Moore, R. E.; Scheuer, P. J.; Paul, V. J. *J. Org. Chem.* **1988**, *53*, 3644; (c) Jefford, C. W.; Bernardinelli, G.; Tanaka, J.; Higa, T. *Tetrahedron Lett.* **1996**, *37*, 159.
- For reviews, see: (a) Crimmins, M. T. *Curr. Opin. Drug Discovery Dev.* **2002**, *5*, 944; (b) Mulzer, J.; Öhler, E. *Chem. Rev.* **2003**, *103*, 3753.
- (a) Mooberry, S. L.; Tien, G.; Hernandez, A. H.; Plubrukarn, A.; Davidson, B. S. *Cancer Res.* **1999**, *59*, 653; (b) Cragg, G. M.; Newman, D. J. *J. Nat. Prod.* **2004**, *67*, 232.
- For an in silico approach to predicting the binding site for laulimalide, see: Pineda, O.; Farràs, J.; Maccari, L.; Manetti, F.; Botta, M.; Vilarrasa, J. *Bioorg. Med. Chem. Lett.* **2004**, *14*, 4825.
- Pryor, D. E.; O'Brate, A.; Bilcer, G.; Diaz, J. F.; Wang, Yu.; Wang, Yo.; Kabaki, M.; Jung, M. K.; Andreu, J. M.; Ghosh, A. K.; Giannakakou, P.; Hamel, E. *Biochemistry* **2002**, *41*, 9109.
- Peloruside has recently been found to bind to the same site as laulimalide: Gaitanos, T. N.; Buey, R. M.; Diaz, J. F.; Northcote, P. T.; Teesdale-Spittle, P.; Andreu, J. M.; Miller, J. H. *Cancer Res.* **2004**, *64*, 5063.
- (a) Ghosh, A. K.; Wang, Y. *J. Am. Chem. Soc.* **2000**, *122*, 11027; (b) Ghosh, A. K.; Wang, Y.; Kim, J. T. *J. Org. Chem.* **2001**, *66*, 8973; (c) Paterson, I.; De Savi, C.; Tudge, M. *Org. Lett.* **2001**, *3*, 213; (d) Paterson, I.; De Savi, C.; Tudge, M. *Org. Lett.* **2001**, *3*, 3149; (e) Mulzer, J.; Öhler, E. *Angew. Chem., Int. Ed.* **2001**, *40*, 3843; (f) Evev, V. S.; Kaehlig, H.; Mulzer, J. *J. Am. Chem. Soc.* **2001**, *123*, 10764; (g) Crimmins, M. T.; Stanton, M. G.; Allwein, S. P. *J. Am. Chem. Soc.* **2002**, *124*, 5958; (h) Williams, D. R.; Mi, L.; Mullins, R. J.; Stites, R. E. *Tetrahedron Lett.* **2002**, *43*, 4841; (i) Nelson, S. G.; Chueng, W. S.; Kassick, A. J.; Hilfiker, M. A. *J. Am. Chem. Soc.* **2002**, *124*, 13654; (j) Wender, P. A.; Hegde, S. G.; Hubbard, R. D.; Zhang, L. *J. Am. Chem. Soc.* **2002**, *124*, 4956.
- (a) Ahmed, A.; Hoegenauer, K.; Enev, V. S.; Hanbauer, M.; Kaehlig, H.; Öhler, E.; Mulzer, J. *J. Org. Chem.* **2003**, *68*, 3026; (b) Wender, P. A.; Hegde, S. G.; Hubbard, R. D.; Zhang, L.; Mooberry, S. L. *Org. Lett.* **2003**, *5*, 3507; (c) Gallagher, B. M., Jr.; Fang, F. G.; Johannes, C. W.; Pesant, M.; Tremblay, M. R.; Zhao, H.; Akasaka, K.; Li, X.-y.; Liu, J.; Littlefield, B. A. *Bioorg. Med. Chem. Lett.* **2004**, *14*, 575; (d) Paterson, I.; Bergmann, H.; Menche, D.; Berkessel, A. *Org. Lett.* **2004**, *6*, 1293; (e) Mooberry, S. L.; Randall-Hlubek, D. A.; Leal, R. M.; Hegde, S. G.; Hubbard, R. D.; Zhang, L.; Wender, P. A. *Proc. Natl. Acad. Sci. U.S.A.* **2004**, *101*, 8803; (f) Gallagher, B. M., Jr.; Zhao, H.; Pesant, M.; Fang, F. G. *Tetrahedron Lett.* **2005**, *46*, 923; (g) Paterson, I.; Menche, D.; Håkansson, A. E.; Longstaff, A.; Wong, D.; Barasoain, I.; Buey, R. M.; Díaz, J. F. *Bioorg. Med. Chem. Lett.*, accepted for publication.
- For some selected examples, see: (a) Taylor, R. E.; Zajicek, J. *J. Org. Chem.* **1999**, *64*, 7224; (b) Snyder, J. P.; Nevins, N.; Cicero, D. O.; Jansen, J. *J. Am. Chem. Soc.* **2000**, *122*, 724; (c) Smith, A. B., III; LaMarche, M. J.; Falcone-Hindley, M. *Org. Lett.* **2001**, *3*, 695; (d) Montegudo, E.; Cicero, D. O.; Cornett, B.; Myles, D. C.; Snyder, J. P. *J. Am. Chem. Soc.* **2001**, *123*, 16929; (e) Paterson, I.; Britton, R.; Delgado, O.; Wright, A. E. *Chem. Commun.* **2004**, *6*, 632.
- Previously, the spectral data of laulimalide have been reported in C₆D₆,^{1a} DMSO^{1b} and CDCl₃.^{1c}

11. Complete spectroscopic data have previously been reported: **1**,¹ **2a**,^{8d} **2b–d**.^{8g}
12. (a) Hoye, T. R.; Hanson, P. R.; Vyvyan, J. R. *J. Org. Chem.* **1994**, *59*, 4096; (b) Hoye, T. R.; Zhao, H. *J. Org. Chem.* **2002**, *67*, 4014.
13. The observed coupling constants in CD₃OD are similar to the ones measured in C₆D₆,^{1a} DMSO^{1b} and CDCl₃,^{1c} which suggest that laulimalide also adopts a similar conformation in these solvents.
14. Mohamadi, F.; Richards, N. G. J.; Guida, W. C.; Kiskamp, R.; Lipton, M.; Caufield, C.; Chang, G.; Hendrickson, T.; Still, W. C. *J. Comput. Chem.* **1990**, *11*, 440.
15. Still, W. C.; Tempczyk, A.; Hawley, R. C.; Hendrickson J. *Am. Chem. Soc.* **1990**, *112*, 6127.
16. Notably, **1-conf 1** is 4.5 kcal mol^{−1} higher in energy than the global minimum as obtained from a non-restrained conformational search under the same conditions.^{8d,g} This sequence is however inverted based on semi-empirical AM1 GAMESS calculations, which suggest **1-conf 1** to be 3 kcal mol^{−1} lower in energy.
17. Berkessel, A.; Menche, D.; Sklorz, C.; Schröder, M.; Paterson, I. *Angew. Chem., Int. Ed.* **2003**, *42*, 1032.
18. For a related approach along these lines, see Ref. 8f.